Post-Cretaceous bursts of evolution along the benthic-pelagic axis in marine fishes

Emanuell Duarte-Ribeiro[1,2], Aaron Davis[3,4], Rafael A. Rivero-Vega[1], Guillermo Ortí[3,5], Ricardo Betancur-R[1,2,3*]

[1]Department of Biology, University of Puerto Rico, Rio Piedras, PO Box 23360, San Juan, Puerto Rico 00931, USA
[2]Department of Biology, The University of Oklahoma, 730 Van Vleet Oval, Room 314, Norman, OK 73019, USA
[3]Department of Vertebrate Zoology, National Museum of Natural History, Smithsonian Institution, PO Box 37012, MRC 159, Washington, DC 20013-7012, USA
[4]Centre for Tropical Water and Aquatic Ecosystem Research (TropWATER), and School of Marine and Tropical Biology, James Cook University, Townsville, Queensland 4811, Australia
[5]Department of Biological Sciences, The George Washington University, 2023 G Street NW, Washington DC 20052, USA

Fossil calibration and divergence time estimation

Our fossil calibration scheme follows Harrington *et al*. [1], but with modifications. Lower bounds of clade age were defined via the minimum age of its earliest fossil representative (calibrations 1-16 below); 95% soft upper bounds were empirically estimated based on the maximum ages of the oldest fossil representatives of successive outgroups for each clade [2]. Monophyly of Pleuronectiformes (ingroup) was assumed (constrained) before analyses, following several recent studies [1,3,4]; placement of outgroup taxa in tree was also constrained based on current knowledge of the Fish Tree of Life [5]. Sequence of outgroups used by Harrington *et al.* [1] to estimate soft upper bounds' 95% confidence intervals: Aulopiformes (hard lower bound: †*Atolvorator longipectoralis*; absolute age estimate: 125 Ma); non-eurypterygian Euteleostei (hard lower bound: †*Leptolepides haerteisi*; absolute age estimate: 150.94 Ma); Otocephala (hard lower bound: †*Tischlingerichthys viholi*; absolute age estimate: 150.94 Ma); Elopomorpha (hard lower bound: †*Anaethalion zapporum*; absolute age estimate: 151.2 Ma); †Ichthyodectiformes (hard lower bound: †*Occithrissops willsoni*; absolute age estimate: 166.1 Ma); †*Leptolepis coryphaenoides* (absolute age estimate: 181.7 Ma); †*Dorsetichthys bechei* (absolute age estimate: 193.81 Ma); †Pholidophoridae (hard lower bound: †*Knerichthys bronni*; absolute age estimate: 221.0 Ma); †*Prohalecites porroi* (absolute age estimate: 236.0 Ma); Holostei (hard lower bound: †*Watsonulus eugnathoides*; absolute age estimate: 247.1 Ma). Hard upper bound was defined based on the stem neopterygian †*Discoserra* (absolute age estimate: 322.8 Ma).

(1) Acanthomorphata. MRCA: *Lampris, Myripristis*. Hard lower bound: †*Aipichthys minor.* Diagnosis and phylogenetic placement: †*Aipichthys minor* is placed on the lampridiform stem based on 67 morphological characters [6]. Stratigraphic horizon and locality: fish beds at Hadjula [7]. Absolute age estimate: 98.0 Ma. 95% soft upper bound: 143.0 Ma. Prior setting: log-normal distribution, mean=2.161, SD=1.0 (crown calibration).

(2) Percomorphaceae + Holocentriformes. MRCA: *Myripristis, Kurtus*. Hard lower bound: †*Stichocentrus liratus.* Diagnosis and phylogenetic placement: enlarged penultimate anal-

fin spine of *Stichocentrus* represents a synapomorphy of holocentroids [8]. Stratigraphic horizon and locality: fish beds at Hadjula [7]. Absolute age estimate: 98.0 Ma. 95% soft upper bound: 128.8 Ma. Prior setting: log-normal distribution, mean=1.782, SD=1.0 (crown calibration).

(3) Syngnathiformes. MRCA: *Mullus, Syngnathus*. Hard lower bound: †*Gasterorhamphosus zuppichini.* Diagnosis and phylogenetic placement: the placement of †*Gasterorhamphosus zuppichini* in Syngnathiformes is supported by the absence of anal-fin spine, enlarged dorsal-fin spine with serrated posterior margin, elongated tubular snout, absence of pleural ribs, enlarged posterodorsal process of cleithrum, rod-like anteroventral process of coracoids and simple pectoral rays [9]. Stratigraphic horizon and locality: "Calcari di Melissano," Porto Selvaggio, Lecce province, Italy. Absolute age estimate: 69.71 Ma. 95% soft upper bound: 98.1 Ma. Prior setting: log-normal distribution, mean=1.6975, SD=1.0 (crown calibration).

(4) Centropomidae (Latinae + Centropominae). MRCA: *Centropomus*, *Lates*. Hard lower bound: †*Eolates gracilis*. Diagnosis and phylogenetic placement: placement of †*Eolates gracilis* in Latiinae is supported by the presence of posterior pad in infraorbital 1 and by having 10+14 vertebrae [10]; †*Eolates gracilis* is the earliest branching lineage of Latiinae [10]. Stratigraphic horizon and locality: early Eocene, upper Ypresian, Monte Bolca, Italy. Absolute age estimate: 49 Ma. 95% soft upper bound: 72.8 Ma. Prior setting: log-normal distribution, mean=1.525, SD=1.0 (crown calibration).

(5) Menidae. MRCA: *Mene, Xiphias*. Hard lower bound: †*Mene purydi.* Diagnosis and phylogenetic placement: †*Mene purydi* has several menid synapomorphies, including a cavernous vault formed by the frontal bones; a pronounced supraoccipital crest ornamented with a distinctive, anteriorly-inclined ridge; well-formed sclerotic ossicles; a lateral plateau on the hyomandibula ornamented with a set of narrow striae; close association of the first and second neural arches [11]. Stratigraphic horizon and locality: northwestern Peru [11]. Absolute age estimate: 55.20 Ma. 95% soft upper bound: 84.7 Ma. Prior setting: log-normal distribution, mean=1.7395, SD=1.0 (crown calibration).

(6) Echeneidae. MRCA: *Remora, Rachycentron*. Hard lower bound: †Echeneidae undet. [12]. Diagnosis and phylogenetic placement: identified as belonging to Echeneidae based on synapomorphies for the family (*e.g.*, a dorsal adhesion disc and expanded transverse processes of vertebrae [12]). Stratigraphic horizon and locality: NP23 - the fish shales of Grube Unterfeld ("Frauenweiler"). Absolute age estimate: 29.62 Ma. 95% soft upper bound: 51.9Ma. Prior setting: log-normal distribution, mean=1.459, SD=1.0 (crown calibration).

(7) Echeneoidei. MRCA: *Echeneis, Scomberoides*. Hard lower bound: †*Ductor vestenae.* Diagnosis and phylogenetic placement: †*Ductor* has been diagnosed either as the sister taxon of crown Echeneoidei, or within crown Echeneoidei as sister to Rachycentridae plus Coryphaenidae. We followed Harington *et al*. [1] opinion and interpreted †*Ductor* as the sister taxon of crown Echeneoidei, as it represents a more conservative application of this fossil placement. Stratigraphic horizon and locality: early Eocene, upper Ypresian, Bolca, Italy. Absolute age estimate: 49 Ma. 95% soft upper bound: 59.1 Ma. Prior setting: log-normal distribution, mean=0.668, SD=1.0 (crown calibration).

(8) Scomberoidini. MRCA: *Scomberoides, Trachnotus*. Hard lower bound: †*Scomberoides spinosus.* Diagnosis and phylogenetic placement: †*Scomberoides spinosus* has been identified as an Scomberoidini based on two synapomorphies: 26 vertebrae [13], and posterior fin rays of the dorsal and anal fin developed as finlets [14]. Stratigraphic horizon and locality: upper Maikop at Chernaya Rechka, Caucasus [15]. Absolute age estimate: 19.30 Ma.

95% soft upper bound: 50.9 Ma. Prior setting: log-normal distribution, mean=1.8082, SD=1.0 (crown calibration).

(9) Carangini. MRCA: *Seriola, Chloroscombrus*. Hard lower bound: †*Eastmanalepes primaevus.* Diagnosis and phylogenetic placement: the presence of scutes along its flank is a synapomorphy of Carangini within Carangidae. Stratigraphic horizon and locality: early Eocene, upper Ypresian, Bolca, Italy. Absolute age estimate: 49 Ma. 95% soft upper bound: 59.1 Ma. Prior setting: log-normal distribution, mean=0.668, SD=1.0 (crown calibration).

(10) Pleuronectiformes. MRCA: *Psettodes, Bothus*. Hard lower bound: †*Heteronectes chaneti.* Diagnosis and phylogenetic placement: *Heteronectes* has been placed as the earliest-branching lineage in the flatfish stem, supported by a set of 58 morphological characters [16]. Stratigraphic horizon and locality: early Eocene, upper Ypresian, Bolca, Italy. Absolute age estimate: 49 Ma. 95% soft upper bound: 72.8 Ma. Prior setting: log-normal distribution, mean=1.525, SD=1.0 (stem calibration).

(11) Bothoid. MRCA: *Symphurus*, *Bothus*. Hard lower bound: †*Eobothus minimus*. Diagnosis and phylogenetic placement: Friedman [16] provides apomorphy-based evidence for placement of †*Eobothus minimus* in Pleuronectoidei. *Eobothus* also shows several derived features (*e.g.*, loss of pelvic-fin spine, anteriorly inclined neural spine of second abdominal vertebra) common to the four 'bothoid' families (Scophthalmidae, Bothidae, Pleuronectidae, and Paralichthyidae). Those characters, however, cannot resolve its relative placement among these lineages [17]. Stratigraphic horizon and locality: early Eocene, upper Ypresian, Bolca, Italy. Absolute age estimate: 49 Ma. 95% soft upper bound: 58.3 Ma. Prior setting: log-normal distribution, mean = 0.648, SD= 1.0 (stem calibration).

(12) Soleidae + Cynoglossidae. MRCA: *Solea*, *Cynoglossus*. Hard lower bound: †*Eobuglossus eocenicus*. Diagnosis and phylogenetic placement: possibly an stem soleid or cynoglossid [9,18]. Stratigraphic horizon and locality: upper Lutetian, Gebel Turah, Egypt [18]. Absolute age estimate: 41.2 Ma. 95% soft upper bound: 52.8 Ma. Prior setting: log-normal distribution, mean=0.815, SD=1.0 (crown calibration). Comment: Near *et al.* [9] placed the calibration one node below (Samaridae + Soleidae + Cynoglossidae) arguing that "Chanet [18] argues that *†Eobuglossus* can be identified as a soleid on the basis of the geometry of the ascending process of the blind side premaxilla. We are not convinced that the state in this fossil can be meaningfully distinguished from the condition found in cynoglossids." A placement of †*Eobuglossus* in the Soleidae + Cynoglossidae crown reconciles both Chanet's [18] and Near et al.'s [9] opinions.

(13) *Scophthalmus*. MRCA: *Scophthalmus, Lepidorhombus*. Hard lower bound: †*Scophthalmus stamatini.* Diagnosis and phylogenetic placement: †*Scophthalmus stamatini* presents features common to Scophthalmidae (*e.g.*, pelvic fins with long insertions that extend on to the urohyal); its placement within *Scophthalmus* is based on the presence of 11 pre-caudal vertebrae [19]. Stratigraphic horizon and locality: fish shales of the lower dysodils exposed near Piatra Neamt, Romania. Absolute age estimate: 29.62 Ma. 95% soft upper bound: 51.3 Ma. Prior setting: log-normal distribution, mean=1.4314, SD=1.0 (crown calibration).

(14) Pleuronectidae. MRCA: *Hypsopsetta*, *Paralichthys*. Hard lower bound: †*Oligopleuronectes germanicus.* Diagnosis and phylogenetic placement: †*Oligopleuronectes* shares two derived features with pleuronectids: it is right-eyed and bears a lateral process on the eye-side frontal [20]. Stratigraphic horizon and locality: lower-Oligocene, Frauenweiler clay-pit, Germany. Absolute age estimate: 29.62 Ma. 95% soft upper bound: 45.8 Ma. Prior setting: log-normal distribution, mean=1.139, SD=1.0 (crown calibration).

(15) Bothidae + *"Cyclopsettidae".* MRCA: *Bothus*, *Cyclopsetta*. Hard lower bound: †*Oligobothus pristinus*. Diagnosis and phylogenetic placement: stem Bothidae based on the presence of myorhabdoi, intermuscular bones with fimbrate proximal and distal ends [19]. Stratigraphic horizon and locality: upper Rupelian, Lower Dysodilic shales, Piatra Neamt, Romania [19]. Absolute age estimate: 29.62 Ma. 95% soft upper bound: 32.6 Ma. Prior setting: log-normal distribution, mean= 0.685, SD=1.0 (crown calibration).

(16) *Bothus*. MRCA: *Bothus*, *Asterorhombus*. Hard lower bound: †*Bothus* sp. Diagnosis and phylogenetic placement: †*Bothus* sp. is diagnosed as a belonging in the genus *Bothus* based on the presence of robust, rectangular haemal spines [21]. Stratigraphic horizon and locality: Middle Tsurevsky Member of the Tsurevsky Formation along the bank of the Psheka River in western North Caucasus [22]. Absolute age estimate: 11.056 Ma. 95% soft upper bound: 32.6 Ma. Prior setting: log-normal distribution, mean= 1.4251, SD=1.0 (crown calibration).

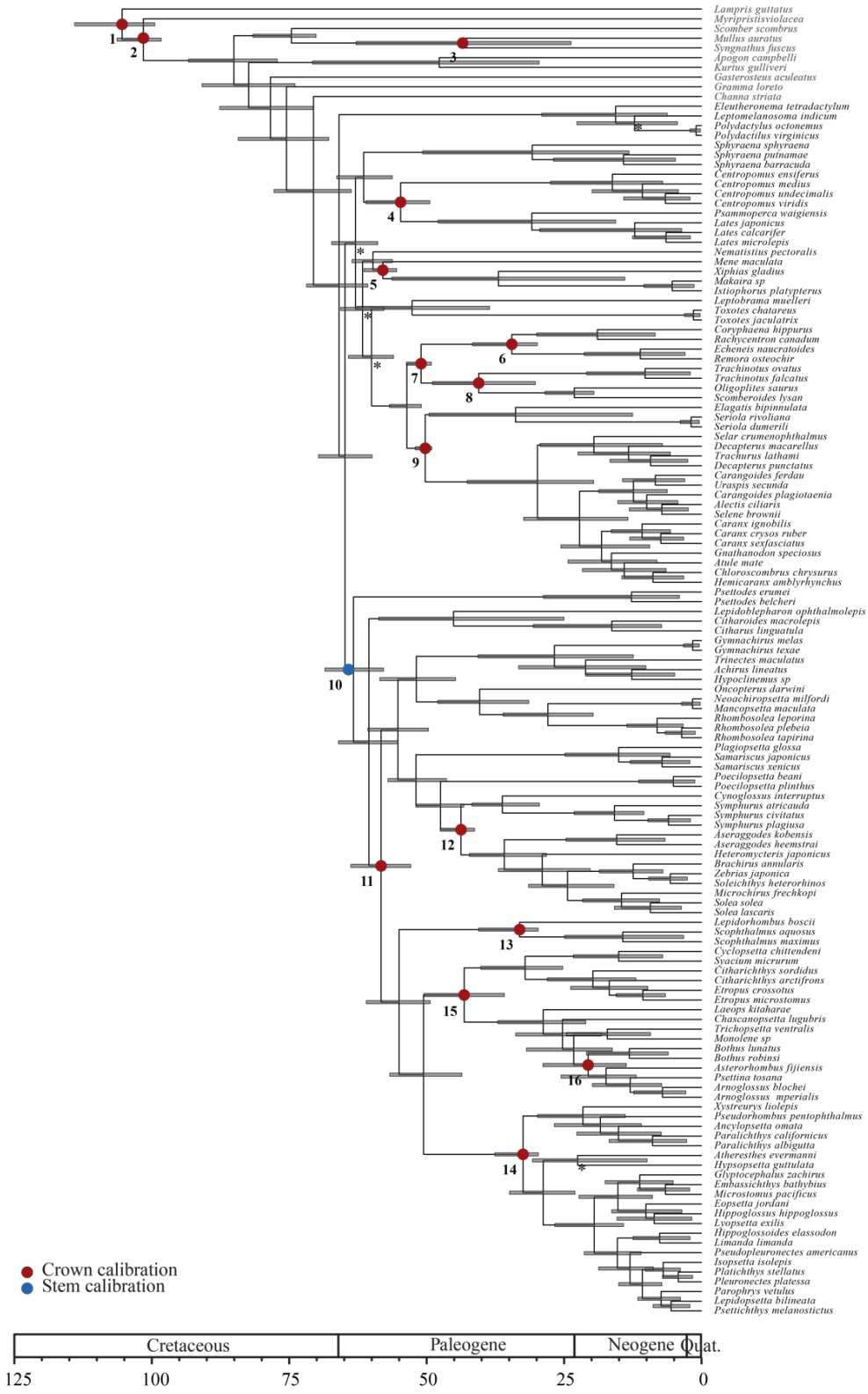

Fig. S1. Maximum Clade Credibility (MCC) tree obtained with BEAST indicating the placement of calibrations used (following the numeration presented above). Bars represent the 95% highest posterior credibility intervals of divergence times. Asterisks (*) indicates nodes with low Bayesian posterior probability support (< 0.70).

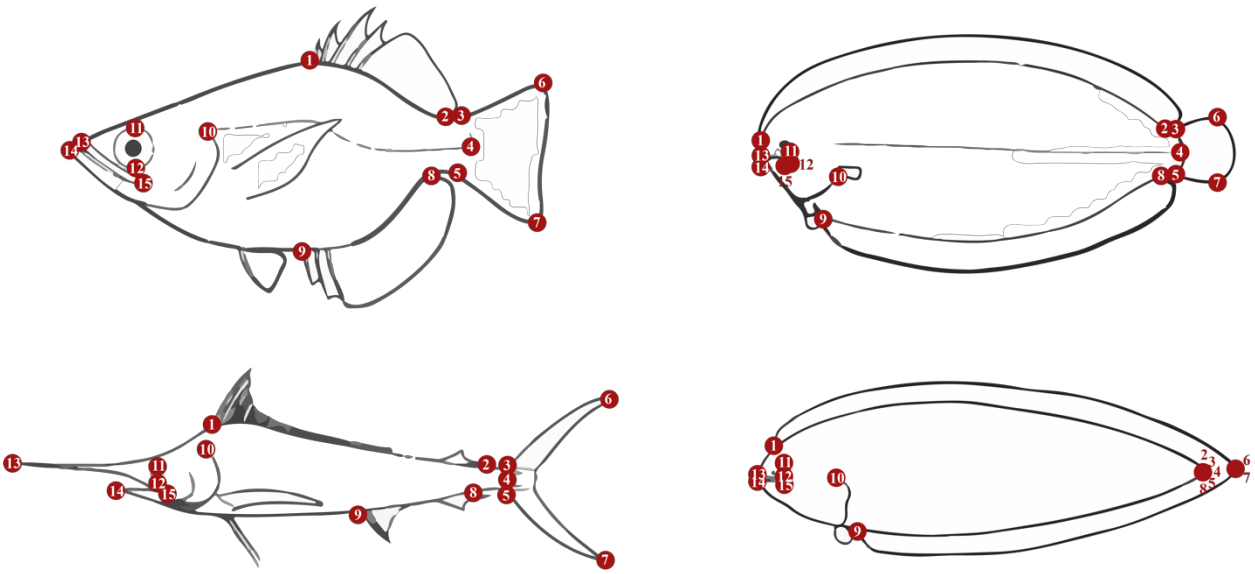

Fig. S2. 15 landmarks selected to summarize body-shape variation in Carangaria. It is based on a set of landmarks generally used to summarize body-shape variation in percomorphs [30,31], and consists in a set of Type I—strictly homologous points—and Type II landmarks—point in which homology is supported by geometric evidence rather than histological data, and are frequently used to describe inflexion points such as the sharpest curvature of a tooth or tips of caudal fin lobes. (1) anterior insertion of dorsal fin, (2) posterior insertion of dorsal fin, (3) dorsal insertion of caudal fin, (4) caudal border of hypural plate aligned with lower lateral line, (5) ventral insertion of caudal fin, (6) posterior end of the most dorsal caudal ray, (7) posterior end of the most ventral caudal ray, (8) posterior insertion of anal fin, (9) anterior insertion of anal fin, (10) dorsal end of the opercula, (11) dorsal margin of the eye, (12) ventral margin of the eye, (13) rostral tip of premaxilla, (14) anterior tip of mandible, and (15) caudal end of maxilla.

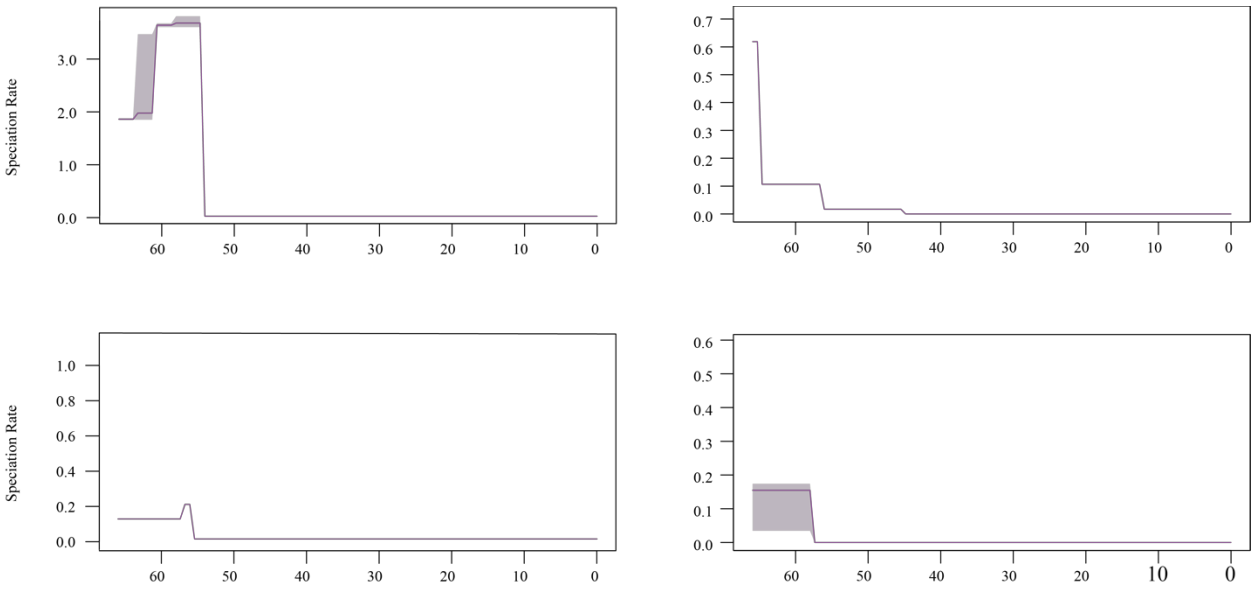

Fig. S3. Rates of speciation through time estimated from the MCC tree using the CoMET function in TESS. Plots highlight the inconsistency of the CoMET results obtained and the high sensitivity of analyses to hyper-prior choice. All analyzes used a minimum threshold value of effective samples (ESS) of 500.

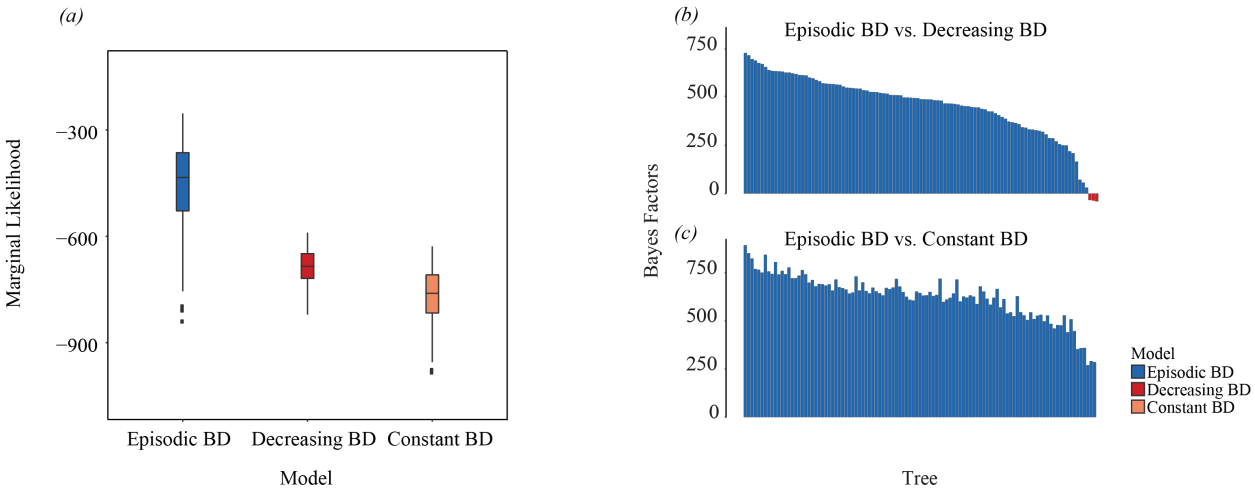

Fig. S4. Model-fit comparisons based on a set of 100 trees evenly sampled from de posterior distribution. Comparisons for alternative models of lineage diversification: (a) distribution of the marginal likelihood for the three alternative branching models; (b) Bayes factors comparing Episodic BD and Decreasing BD models for the 100 resampled trees; and (c) Bayes factors comparing Episodic BD and Constant BD for the 100 resampled trees

Assessing the robustness of lineage diversification analyses based on multiple taxonomic sampling schemes and other alternative statistics

We assessed whether our limited taxonomic sampling has affected the lineage diversification analyses by performing a sequence of posterior-predictive simulations to test the absolute fit of candidate models to our data. Posterior-predictive simulations (as implemented in TESS) follow a series of steps that start with a MCMC simulation to estimate the posterior probability distribution of diversification parameters of the candidate models based on our observed dataset. The rate parameters (e.g., speciation, extinction) from the joint posterior densities, as well as priors initially used in the rate parameter estimations (e.g., sampling fraction, sampling strategy), are then used to parameterize models and simulate trees. Once these trees are simulated, the summary statistics calculated for the observed dataset are compared to the posterior-predictive distribution.

We compared the cladogenesis patterns observed in the Lineage Through Time (LTT) plots generated using the empirical tree against patterns generated using trees simulated under the three candidate models we initially used for model fitting in TESS: Constant BD, Decreasing BD, and Episodic BD (see methods for a more detailed description of the competing models). Comparisons between the LTT accumulation generated using the empirical tree show a clear deviation to the pattern expected under a Constant BD model (Fig. S5), with significantly negative values of γ (-2.99, P = 0.002). No significant deviation was observed between the LTT accumulation curve generated using the empirical tree and the patterns generated under Decreasing BD and Episodic BD, which indicates agreement with the model fitting analysis and supports a time-heterogeneous process as an explanation for the lineage diversification in Carangaria. The two time-heterogeneous models present similar patterns of lineage accumulation and resemble the pattern obtained with the empirical tree—a steep curve representing an initial burst of diversity accumulation followed by a period of lower rates of diversification. Therefore, both can be used to simulate trees with cladogenesis patterns similar to the ones observed in the empirical tree, providing a good absolute fit to our dataset. Note that the final selection between these two models follows the model-fitting test presented in the main text.

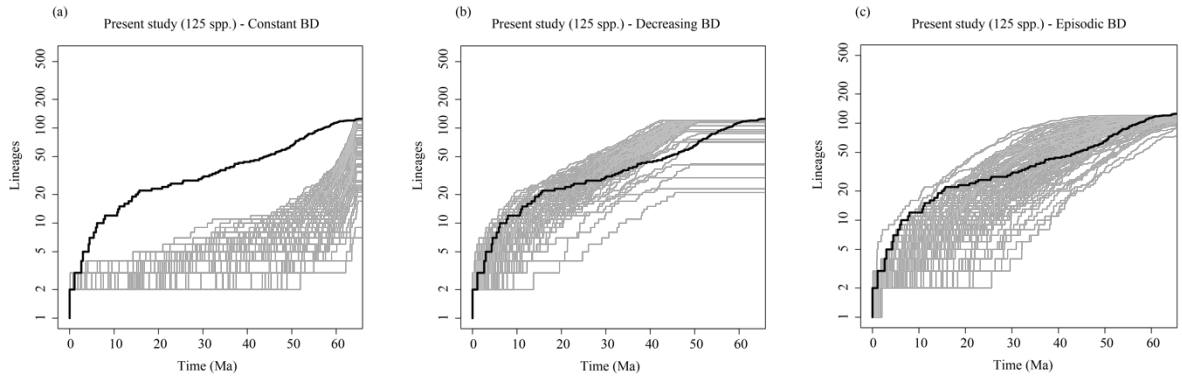

Fig. S5. Assessing the absolute fit of the MCC tree to the competing models of lineage diversification using posterior-predictive simulation. Black lines represent the pattern of Lineage accumulation Through Time (LTT) for the MCC tree while gray lines show LTT curves for the simulated trees under (*a*) Constant BD, (*b*) Decreasing BD, and (*c*) Episodic BD.

To further test whether the limited taxonomic sampling scheme may affect our lineage diversification analyses, we expanded the predictive simulation analyses to four alternative phylogenetic scenarios: (1) a 45-taxa tree (from Harrington et al. [1]); (2) a 405-taxa supermatrix tree (from Rabosky et al. [23]); (3) a 508-taxa grafted tree obtained by adding two well-sampled carangarian subclades (carangoids [24] and flatfishes [25]) into the Rabosky et al. [23] backbone tree; and (4) a 1006-taxa imputed tree from Rabosky et al. [23], which was populated with simulated taxa in place of missing tips. Note that the grafted tree does not intend to provide a new phylogenetic hypothesis for Carangaria; instead, it provides a synthesis of our current knowledge of their phylogeny and divergence times into the extended phylogenetic tree assembled by Rabosky et al. [23]. Additionally, crown ages for major Carangaria groups varies substantially among the independently estimated time trees. To address this issue, we recalibrated those trees by adjusting Carangaria's crown group age to reflect the age obtained in our analysis (see details in Table S5). In all cases, lineage accumulation scenarios resemble the pattern obtained by the exponentially Decreasing BD model (Fig. S6). Therefore, this model also presents a good absolute fit to the alternative datasets regardless of taxonomic sampling schemes used.

Finally, we used the aforementioned, independently estimated phylogenetic hypotheses to generate lineage-through-time (LTT) plots and to estimate the Lineage Diversification Index (LDI) statistic [23]. These statistics provides an alternative avenue to examine whether the cladogenetic history of Carangaria is better explained by pure-birth (LDI ~0), early burst (positive LDIs), or recent speciation (negative LDIs) processes. As expected, and regardless of the taxonomic coverage, all alternative sampling schemes present positive LDI values (ranging from 0.24 to 0.83; Fig. S7). These results indicate that an early burst of diversification represents the most likely diversification scenario for the clade, strongly suggesting that our analyses remain unaffected by the use of alternative trees and methods.

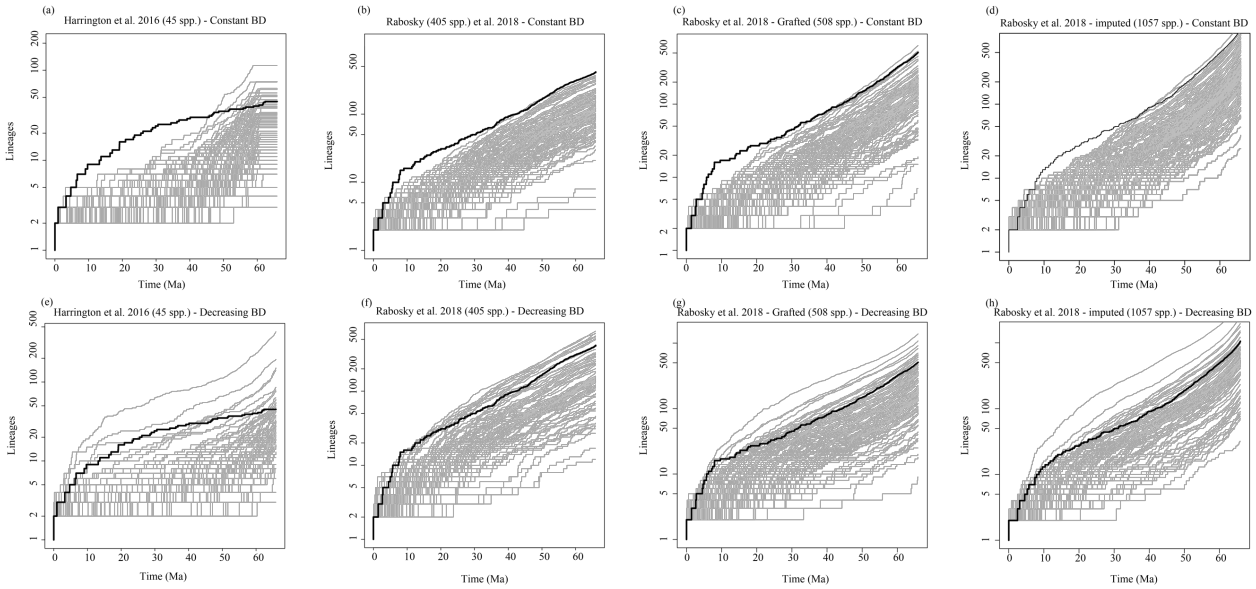

Fig. S6. Predictive simulation results under Constant BD and Decreasing BD for four alternative (independently estimated) time trees that incorporate different taxonomic sampling schemes (45 to 1057 tips). (*a,e*) 45-taxa tree derived from Harrington et al. [1]; (*b,f*) 405-taxa tree from Rabosky et al. [23]; (*c,g*) 508-taxa grafted tree based on Rabosky et al. [23]; and (*d,h*) 1006-taxa imputed tree from Rabosky et al. [23].

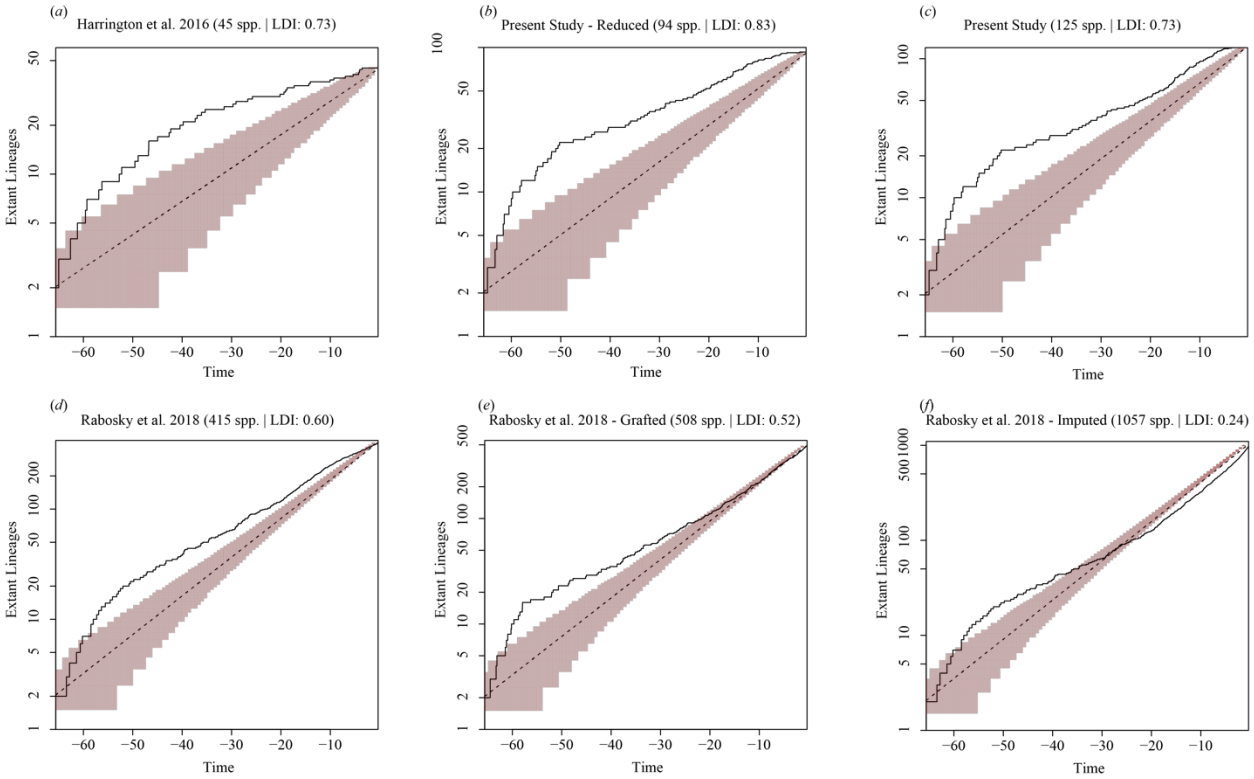

Fig. S7. Lineage Diversification Index (LDI) statistic for six alternative time trees that incorporate different taxonomic sampling schemes: (*a*) 45-taxa tree derived from Harrington et al. [1]; (*b*) our 125-taxa MCC tree; (c) 95-taxa pruned version of our MCC tree that excludes recent cladogenetic events, leaving only one species per genus; (*d*) 405-taxa tree from Rabosky et al. [23]; (*e*) 508-taxa grafted tree based on Rabosky et al. [23]; and (*f*) 1006-taxa imputed tree from Rabosky et al. [23].

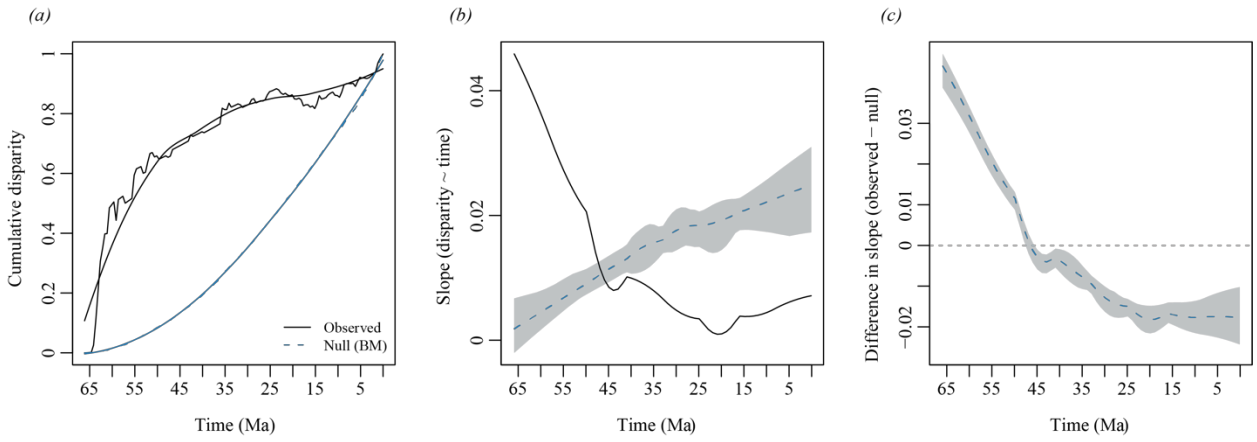

Fig. S8. Disparity-through time plots showing the evolution of morphospace filling in Carangaria using the 5% threshold trait dataset (the highest 4 pPC axes). (a) Accumulation of multivariate disparity through time in 1Myr time slices (thick black line, observed data; thin black line, after LOESS (locally estimated scatterplot smoothing) smoothing; blue lines, constant rate Brownian motion null model). (b) Comparison of slopes for the two competing models; shaded areas represent 95% confidence intervals. (c) Differences in slope for the observed data and the BM null model; values above and below zero indicate dominance of morphospace expansion versus morphospace

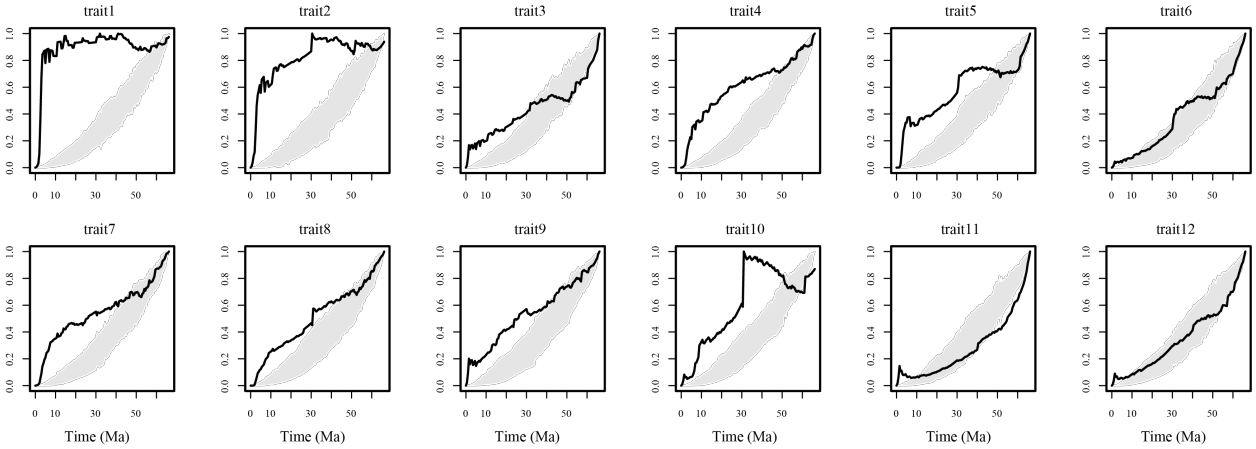

Fig. S9. Accumulation of disparity through time for the first 12 phylogenetically corrected PC axis (pPCA). Black lines represent observations; shaded areas show the 95% confidence intervals of the constant rate Brownian motion model.

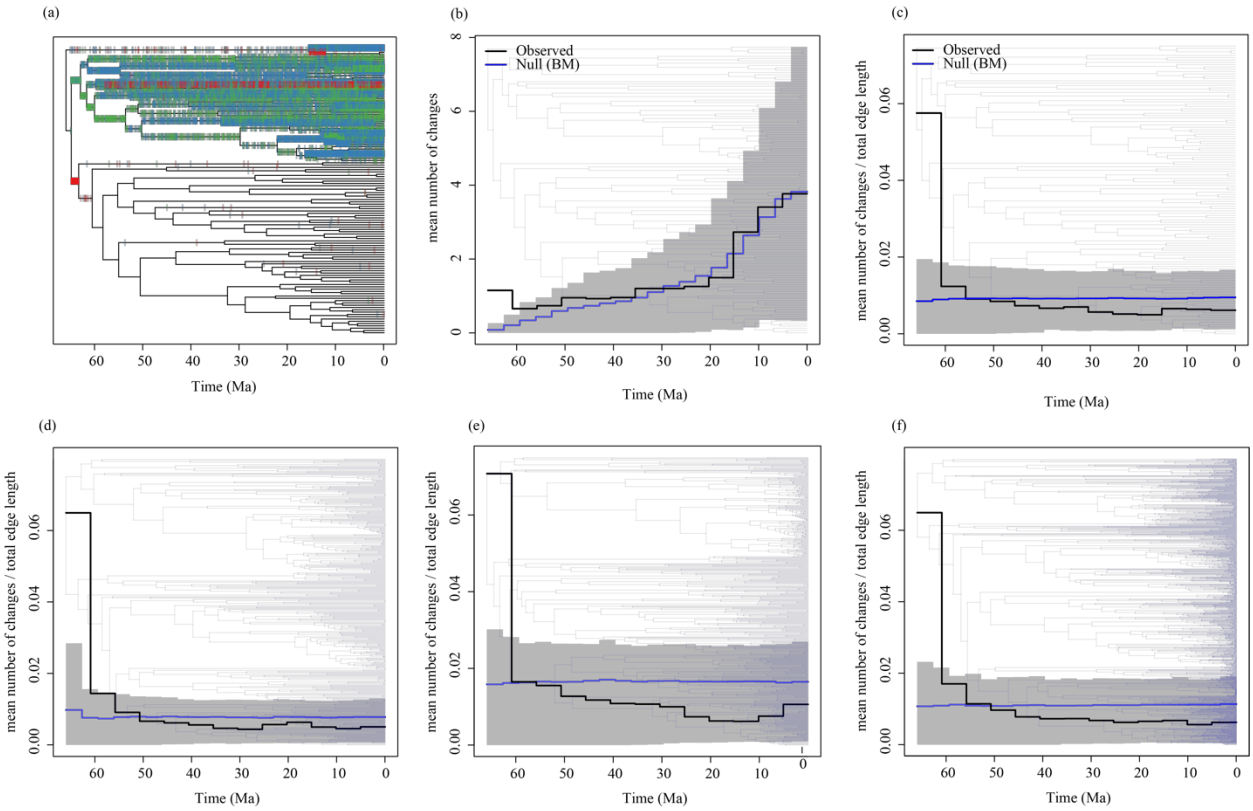

Fig. S10. Habitat transitions though time. (*a*) Stochastic mapping of ecological transitions calculated from 1000 SIMMAP replicates on the maximum clade credibility tree. (*b*) Average number of changes for in 5 Myr slices (black line represents observations; blue lines indicate mean values for the null expectations under a constant rate of character evolution; shaded area represents the 95% confidence intervals). (*c*) Rate of habitat transitions in 5 Myr time slices—mean number of changes per time segment, divided by the total edge length encompassed by the segment. (*d*) Rate of habitat transition based on a 402-taxa tree for Carangaria estimated by Rabosky et al. [22] using supermatrix analyses (after pruning tips without available habitat occupation data); 508-taxa based on Rabosky et al. backbone tree, after grafting two well-sampled Carangaria subclades (carangoids [32] and flatfishes [33]); and (*e*) 1006 tips based on Rabosky et al. backbone tree, further populated with simulated placement for missing tips using imputation methods.

Table S1. See supplementary spreadsheet.

Table S2. TESS model-fit comparisons using the MCC tree.

		Bayes Factors vs.		
	Marginal Likelihood	Episodic BD	Decreasing BD	Constant BD
Episodic BD	-331.71	0	1011.65	1017.73
Decreasing BD	-837.54	-1011.65	0	6.07
Constant BD	-840.57	-1017.73	-6.07	0

Table S3. mvMORPH model-fit comparisons using the MCC tree and the 1% threshold trait subset (the highest 12 pPC axes).

Model	Rank	AIC	diff	AICw
EBOUi	1	-6755	0	1
BMOUi	2	-6746	9.02	0.011
OU	3	-6589	166.32	0
EBBMi	4	-6300	455.29	0
BM	5	-6297	458.46	0
EB	6	-6250	505.07	0

Table S4. mvMORPH model-fit comparisons using the MCC tree and the 5% threshold trait subset (the highest 4 pPC axes).

Model	Rank	AIC	diff	AICw
EBOUi	1	-1877	0	0.9604
BMOUi	2	-1871	6.38	0.0396
OU	3	-1746	131.25	0
EBBMi	4	-1644	233.32	0
BM	5	-1609	268.23	0
EB	6	-1599	278.67	0

Table S5. Comparison of age estimates by multiple (and in many cases independent) phylogenetic studies. With the exception of the Rabosky et al. [22] date inference, which appears overestimated, all other estimates for the crown age of Carangaria are in line with the results obtained here.

Study	Mean crown age	95% HPD
This study	67 Ma	(62-72 Ma)
Alfaro et al. [24]	69 Ma	(64-75 Ma)
Betancur-R. et al. [25]	73 Ma	-
Betancur-R. et al. [5]	65 Ma	(58-75 Ma)
Near et al. [26]	73 Ma	-
Hughes et al. [27]	69 Ma	(63-77 Ma)
Harrington et al. [1]	70 Ma	(64-78 Ma)
Rabosky et al. [28]	83 Ma	-
Chen et al. [29]	73 Ma	(56-81 Ma)

References

1. Harrington RC, Faircloth BC, Eytan RI, Smith WL, Near TJ, Alfaro ME, Friedman MA. 2016 Phylogenomic analysis of carangimorph fishes reveals flatfish asymmetry arose in a blink of the evolutionary eye. *BMC Evol. Biol.* , 1–14. (doi:10.1186/s12862-016-0786-x)
2. Hedman MM. 2010 Constraints on clade ages from fossil outgroups. *Paleobiology* **36**, 16–31. (doi:10.1666/0094-8373-36.1.16)
3. Betancur-R. R *et al.* 2013 Addressing Gene Tree Discordance and Non-Stationarity to Resolve a Multi-Locus Phylogeny of the Flatfishes (Teleostei : Pleuronectiformes). *Syst. Biol.* **62**, 763–785. (doi:10.1093/sysbio/syt039)
4. Betancur-R R, Ortí G, Betancur-R. R, Ortí G. 2014 Molecular evidence for the monophyly of flatfishes (Carangimorpharia: Pleuronectiformes). *Mol. Phylogenet. Evol.* **73**, 18–22. (doi:10.1016/j.ympev.2014.01.006)
5. Betancur-R. R *et al.* 2013 The Tree of Life and a New Classification of Bony Fishes. *PLOS Curr. Tree Life* **Apr 18**, 1–45. (doi:10.1371/currents.tol.53ba26640df0ccaee75bb165c8c26288)
6. Davesne D, Friedman M, Barriel V, Lecointre G, Janvier P, Gallut C, Otero O. 2014 Early fossils illuminate character evolution and interrelationships of Lampridiformes (Teleostei, Acanthomorpha). *Zool. J. Linn. Soc.* (doi:10.1111/zoj.12166)
7. Benton MJ, Donoghue PCJ, Asher RJ, Friedman M, Near TJ, Vinther J. 2015 Constraints on the timescale of animal evolutionary history. *Palaeontol. Electron.*
8. Patterson C. 1993 An overview of the early fossil record of acanthomorphs. *Bull. Mar. Sci.* **52**, 29–59.
9. Near TJ, Eytan RI, Dornburg a., Kuhn KL, Moore J a., Davis MP, Wainwright PC, Friedman M, Smith WL. 2012 Resolution of ray-finned fish phylogeny and timing of diversification. *Proc. Natl. Acad. Sci.* **109**, 13698–13703. (doi:10.1073/pnas.1206625109)
10. Otero O, Otero O. 2004 Anatomy, systematics and phylogeny of both Recent and fossil latid shes (Teleostei, Perciformes, Latidae). *Society* , 81–133. (doi:10.1111/j.1096-3642.2004.00111.x)
11. Friedman M, Johnson GD. 2005 A New Species of Mene (Perciformes: Menidae) from the Paleocene of South America, with Notes on Paleoenvironment and a Brief Review of Menid Fishes. *J. Vertebr. Paleontol.* **25**, 770–783. (doi:10.1671/0272-4634(2005)025[0770:ANSOMP]2.0.CO;2)
12. Friedman M, Johanson Z, Harrington RC, Near TJ, Graham MR. 2013 An early fossil remora (Echeneoidea) reveals the evolutionary assembly of the adhesion disc. *Proc. Biol. Sci.* **280**, 20131200. (doi:10.1098/rspb.2013.1200)
13. Smith-Vaniz WF. 1984 Carangidae: relationships. In *Ontogeny and Systematics of Fishes*, pp. 522–530.
14. Bannikov AF. 1990 Fossil carangids and apolectids of the USSR. *Tr. Paleontol. Instituta* , 1–106.
15. Bannikov AF, Parin NN. 1997 The list of marine fishes from Cenozoic (Upper Paleocene-Middle Miocene) localities in Southern European Russia and adjacent countries. *J. Ichthyol.*
16. Friedman M. 2008 The evolutionary origin of flatfish asymmetry. *Nature* **454**, 209–212. (doi:10.1038/nature07108)

17. Hoshino K. 2001 Monophyly of the Citharidae (Pleuronectoidei: Pleuronectiformes: Teleostei) with considerations of pleuronectoid phylogeny. *Ichthyol. Res.* (doi:10.1007/s10228-001-8163-0)
18. Chanet B. 1994 Eobuglossus eocenicus (Woodward , 1910) from the Upper Lutetian of Egypt , one of the oldest soleids [Teleostei , Pleuronectiformi]. *Neues Jahrb. für Geol. und Paläontologie*
19. Baciu DS, Chanet B. 2002 Les Poissons plats fossiles (teleostei: Pleuronectiformes) de l'Oligocène de Piatra neamt (Roumanie). *Oryctos* **4**, 17–38.
20. Sakamoto K, Uyeno T, Micklich N. 2004 Oligopleuronectes germanicus gen. et. sp. nov., an Oligocene pleuronectid from Frauenweiler, S. Germany. *Bull. Natl. Sci. Museum, Tokyo* **C 30**, 89–94.
21. Chanet B, Sorbini C. 2001 A male fish Bothus podas (Delaroche, 1809)[Pleuronectiformes: Bothidae] in the Pliocene of the Marecchia river (Italy). *BOLLETTINO-SOCIETA Paleontol. Ital.* **40**, 345–350.
22. Carnevale G, Bannikov AF, Landini W, Sorbini C. 2006 Volhynian (early Sarmatian sensu lato) fishes from Tsurevsky, North Caucasus, Russia. *J. Paleontol.* (doi:10.1666/0022-3360(2006)80[684:vesslf]2.0.co;2)
23. Harmon LJ, Schulte JA, Larson A, Losos JB. 2003 Tempo and mode of evolutionary radiation in iguanian lizards. *Science (80-.).* (doi:10.1126/science.1084786)
24. Alfaro ME, Faircloth BC, Harrington RC, Sorenson L, Friedman M, Thacker CE, Oliveros CH, Černý D, Near TJ. 2018 Explosive diversification of marine fishes at the Cretaceous–Palaeogene boundary. *Nat. Ecol. Evol.* , 1–9. (doi:10.1038/s41559-018-0494-6)
25. Betancur-R R, Wiley EO, Arratia G, Acero A, Bailly N, Miya M, Lecointre G, Ortí G. 2017 Phylogenetic classification of bony fishes. *BMC Evol. Biol.* **17**, 162. (doi:10.1186/s12862-017-0958-3)
26. Near TJ *et al.* 2013 Phylogeny and tempo of diversification in the superradiation of spiny-rayed fishes. *Proc. Natl. Acad. Sci. U. S. A.* **110**, 12738–12743. (doi:10.5061/dryad.d3mb4)
27. Hughes LC *et al.* 2018 Comprehensive phylogeny of ray-finned fishes (Actinopterygii) based on transcriptomic and genomic data. *Proc. Natl. Acad. Sci.* , 201719358. (doi:10.1073/pnas.1719358115)
28. Rabosky DL *et al.* 2018 An inverse latitudinal gradient in speciation rate for marine fishes. *Nature* **559**, 392–395. (doi:10.1038/s41586-018-0273-1)
29. Chen W-J, Santini F, Carnevale G, Chen J-N, Liu S-H, Lavoue S, Mayden RL. 2014 New insights on early evolution of spiny-rayed fishes (Teleostei: Acanthomorpha). *Front. Mar. Sci.* **1**, 53. (doi:10.3389/fmars.2014.00053)
30. Chakrabarty P. 2005 Testing Conjectures about Morphological Diversity in Cichlids of Lakes Malawi and Tanganyika. *Copeia* **2005**, 359–373. (doi:10.1643/CG-04-089R2)
31. Friedman M. 2010 Explosive morphological diversification of spiny-finned teleost fishes in the aftermath of the end-Cretaceous extinction. *Proc. R. Soc. B Biol. Sci.* **277**, 1675–1683. (doi:10.1098/rspb.2009.2177)
32. Santini F, Carnevale G. 2015 First multilocus and densely sampled timetree of trevallies, pompanos and allies (Carangoidei, Percomorpha) suggests a Cretaceous origin and Eocene radiation of a major clade of piscivores. *Mol. Phylogenet. Evol.* **83**, 33–39. (doi:10.1016/j.ympev.2014.10.018)
33. Byrne L, Chapleau F, Aris-brosou S. 2018 How the Central American Seaway and an

ancient northern passage affected f latfish diversification.
(doi:10.1093/molbev/msy104/5000153)